Pang Yuxi (Orcid ID: 0000-0001-5039-0236)

An efficient $R_{1\rho}$ dispersion imaging method for human knee cartilage using constant magnetization prepared turbo-FLASH

[1]Yuxi Pang, PhD, [2,3]Riann M. Palmieri-Smith, PhD and [3]Tristan Maerz, PhD.

[1]Department of Radiology, University of Michigan, Ann Arbor, Michigan, USA; [2]School of Kinesiology and [3]Department of Orthopaedic Surgery, University of Michigan, Ann Arbor, Michigan, USA.

Corresponding Author:

Yuxi Pang, PhD
Department of Radiology, University of Michigan,
1500 E. Medical Center Dr., Ann Arbor, MI 48109-5030
Tel: 734-232-6585
Fax: 734-764-2412
Email: yuxipang@umich.edu
Twitter: @yuxipang
ORCID iD: Yuxi Pang (https://orcid.org/0000-0001-5039-0236)

Running Title: An efficient R1ρ dispersion imaging of human knee cartilage

This is the author manuscript accepted for publication and has undergone full peer review but has not been through the copyediting, typesetting, pagination and proofreading process, which may lead to differences between this version and the Version of Record. Please cite this article as doi: 10.1002/nbm.4500

Word Count: 5,110

ABSTRACT

This work aimed to develop an efficient $R_{1\rho}$ dispersion imaging method for clinical studies of human knee cartilage at 3T. Eight constant magnetizations (M_{prep}) were prepared by tailoring both the duration and amplitude (ω_1) of a fully-refocused spin-lock preparation pulse. The limited M_{prep} dynamic range was expanded by the measure, equivalent to that with ω_1=∞, from the magic angle location in the deep femoral cartilage. The developed protocol with M_{prep}=60% was demonstrated on one subject's bilateral and two subjects' unilateral asymptomatic knees. The repeatability of the proposed protocol was estimated by two repeated scans with a three-month gap for the last two subjects. The synthetic $R_{1\rho}$ and R_2 derived from $R_{1\rho}$ dispersions were compared with the published references using the state-of-the-art $R_{1\rho}$ and R_2 mapping (MAPSS). The proposed protocol demonstrated good (<5%) repeatability quantified by the intra- and inter-subject's coefficient of variations in the femoral and tibial cartilage. The synthetic $R_{1\rho}$ (1/s) and the references were comparable in the femoral (23.0±5.3 vs. 24.1±3.8, *P*=.67) and the tibial (29.1±8.8 vs. 27.1±5.1, *P*=.62), but not the patellar (16.5±4.9 vs. 22.7±1.6, *P*<.01) cartilage. The same

trends were also observed for the current and the previous R_2. In conclusion, the developed $R_{1\rho}$ dispersion imaging scheme has been revealed not only efficient but also robust for clinical studies of human knee cartilage at 3T.

Key words: Quantitative $R_{1\rho}$ dispersion imaging, tailored constant $R_{1\rho}$ weighting, turbo-FLASH, fully-refocused spin-lock preparation, magic angle effect, human knee articular cartilage.

Abbreviations: CV, coefficient of variation; CV_{rms}, root-mean-square of CVs; DZ, deep zone; FA, flip angle; FLASH, fast low angle shot; FOV, field of view; HR, hit rate; MA, magic angle; MAPSS, magnetization-prepared angle-modulated partitioned k-space spoiled gradient echo snapshots; M_{prep}, spin-lock prepared magnetization; PG, proteoglycan; REF, internal reference; RF, radio frequency; ROI, region of interest; SENSE, sensitivity encoding; SL, spin-lock; SZ, superficial zone; TSL, spin-lock time; μs, microsecond;

1 | INTRODUCTION

Water proton MR relaxation is not only an important factor governing an exquisite soft-tissue contrast in clinical MR imaging,[1] but it also becomes a powerful tool for studying in detail the structural and dynamic information about biological tissues.[2-4] One of such parameters is the longitudinal relaxation ($T_{1\rho}$=1/$R_{1\rho}$) in a rotating frame, which has been demonstrated to provide unique insights into water-macromolecule interactions.[5-8] The

observed relaxation rate $R_{1\rho}$ depends predominantly on a spin-lock (SL) amplitude ω_1; in other words, $R_{1\rho}$ varies with ω_1 - a well-known phenomenon referred to as $R_{1\rho}$ dispersion in the literature.[5,8] As early as 1970s, $R_{1\rho}$ dispersion had been utilized for investigating pathophysiological changes in biological samples.[5] Two decades later, the first $R_{1\rho}$ imaging study on articular cartilage degeneration was reported,[9] and since then, considerable efforts have been devoted to developing and standardizing $R_{1\rho}$ mapping methodology across primary MR system platforms in clinical settings.[8,10-13]

$R_{1\rho}$ could be viewed as a specific transverse relaxation rate (R_2) under the influence of an applied SL RF pulse, and it is particularly sensitive to low-frequency water molecular interactions.[5,7,14] $R_{1\rho}$ mapping of articular cartilage has been motivated by the diagnostic utility of a noninvasive and sensitive imaging method that can detect early cartilage degeneration in the absence of structural changes apparent on standard MR imaging.[11,15-17] Since $R_{1\rho}$ was first proposed as a promising MR biomarker for characterizing changes in proteoglycan (PG) content, the specificity of its changes with PG alterations has not been well understood.[8,15,18] The existing preclinical and clinical evidences suggest that $R_{1\rho}$ itself is not specifically sensitive to PG alterations, but rather $R_{1\rho}$ dispersion is predominantly susceptible to collagen changes, which are characterized by the residual dipolar interaction of some ordered water molecules buried inside of collagen triple-helical microstructures.[7,8,19,20] These observations are in accordance with two previous studies

from early 2000s[21,22] as well as with some recent investigations relevant to the underlying $R_{1\rho}$ relaxation mechanisms in cartilage.[19,20,23]

Recently, a theoretical framework of $R_{1\rho}$ dispersion in cartilage has been outlined,[7] suggesting that an orientation-independent MR metric, named order parameter S[24], can be derived for detecting early collagen degeneration in joint osteoarthritis. Traditionally, $R_{1\rho}$ dispersion profile was obtained by collecting a series of $R_{1\rho}$ mapping by varying ω_1, with each $R_{1\rho}$ mapping in turn being created from another series of $R_{1\rho}$-weighted images with varying SL durations (TSL).[7,8,25] As demonstrated schematically in Figure 1c, the standard $R_{1\rho}$ dispersion imaging (white dots) takes an unrealistically long acquisition time; thus, it is deemed to be impractical for clinical studies.

Apart from a lengthy acquisition time, it is also challenging to persistently obtain a reliable $R_{1\rho}$ under various ω_1 conditions using a magnetization-prepared spoiled turbo-FLASH sequence.[17,26,27] The potential $R_{1\rho}$ quantification errors could be introduced during SL preparation and/or during imaging readout. It has been well documented that the prepared SL magnetization (M_{prep}) is highly susceptible to B_0 and B_1 non-uniform field artifacts.[28-32] Although many advanced SL schemes, including those using adiabatic pulses, have been developed in the past, none of these methods was specifically designed or optimized for $R_{1\rho}$ dispersion imaging using a broad range of ω_1.

The prepared M_{prep}, on the other hand, could be further compounded by an adverse T_1 relaxation effect, stemmed from the prepared transient signal evolution towards steady-

state during imaging readout.[17,27] To mitigate this detrimental effect, advanced pulse sequences including RF phase cycling and tailored excitation flip angles (FA) have been proposed;[17,33] however, these advanced techniques are not suitable for clinical $R_{1\rho}$ dispersion imaging because of a twofold increase of acquisition time as well as the complexity in tailoring FA schemes.

To further explore $R_{1\rho}$ dispersion of articular cartilage in clinical studies, there exists an unmet need to develop a reliable acquisition protocol without substantially increasing the imaging time. Hence, the aim of this work was to develop a practical $R_{1\rho}$ dispersion imaging method for clinical studies of the human knee cartilage. The proposed protocol was evaluated on four human asymptomatic knees from three adult volunteers at 3T, and the results were compared with those measured with the state-of-the-art $R_{1\rho}$ mapping sequences (MAPSS) in the literature.[17]

2 | METHODS

2.1 | Constant $R_{1\rho}$ weighting using tailored TSL and ω_1

An image voxel signal, $S(TSL, \omega_1)$, from $R_{1\rho}$-weighted image of cartilage[7] can be expressed using Eqs. 1-2,

$$S(TSL, \omega_1) = S_0 \exp(-R_{1\rho} * TSL) \qquad (1)$$

$$R_{1\rho} = R_2^i + \frac{R_2^{ex}}{1+4\omega_1^2\tau_{ex}^2} + \frac{R_2^a(\theta)}{1+4\omega_1^2\tau_b^2} \qquad (2)$$

where S_0, R_2^i, R_2^a and R_2^{ex} denote respectively an initial signal, an isotropic and an anisotropic dipolar relaxation rates, and a chemical exchange induced relaxation rate. Here, the chemical exchange time and the anisotropic dipolar interaction correlation time are represented by τ_{ex} and τ_b, respectively. Note, R_2^{ex} contributes only a few percent to $R_{1\rho}$ in cartilage at 3T, and thus it can be safely disregarded from Eq. 2.[7,8] Accordingly, R_2^{ex} was set to zero in this work unless stated otherwise.

$R_2^a(\theta)$ is normally written as $R_2^a\langle 3cos^2\theta - 1\rangle^2/4$, with θ an angle between the collagen fiber primary direction in the deep femoral cartilage and B_0;[7,34] consequently, $R_{1\rho}$ will become R_2^i when θ=54.7°, the so-called magic angle (MA). On the other hand, the same result can also be obtained when ω_1=∞. This fact had been exploited herein to increase the limited dynamic range in the prepared M_{prep}, defined as $\exp(-R_{1\rho} * TSL)$. More specifically, the signal derived from θ=54.7° in the deep femoral cartilage was treated as that with ω_1=∞. This extra information, i.e. $S_0\exp(-R_2^i * TSL)$, has been referred to as an internal reference (REF) in the literature.[23]

To our knowledge, only two quantitative $R_{1\rho}$ dispersion investigations on the human knee cartilage *in vivo* at 3T have been reported in the past.[7,25] The so-called inflection point (ω_{ip}) on $R_{1\rho}$ dispersion curve is determined by setting the second derivative of Eq. 2 to zero, leading to the relationship of $1/\tau_b = 2\sqrt{3}\omega_{ip}$. An average τ_b of 262±58 (μs) could be thus obtained based on the reported ω_{ip} values,[25] consistent with the previous estimation.[7] Hence, τ_b of 300 (μs) was chosen for numerical simulations in this

work. Additionally, R_2^i and R_2^a were estimated to be 20 (1/s) based on the measured $R_{1\rho}$ dispersion profiles in Figure 3A from the original paper.[25] Given all these assumed values, a specific M_{prep} can be calculated by a judicious combination of TSL and ω_1 in Eqs. 1-2 (see Figure 1c). One constant M_{prep} of 60% was prepared and tabulated in Table 1, containing eight pairs of TSL and $\omega_1/2\pi$, with the former ranging from 13 to 24 ms and the latter from 0 to 1 kHz.

2.2 | A practical $R_{1\rho}$ dispersion imaging protocol

To ensure a reliable prepared M_{prep} that can be subsequently measured as much as possible during imaging readout, an improved SL preparation and an optimal FA (see below) in FLASH sequence were implemented for the proposed $R_{1\rho}$ dispersion imaging method. A pair of refocusing RF pulses (180°) were inserted in the middle of two pairs of antiphase rotary-echo pulses as sketched in Figure 1a, leading to fully refocusing the chemical shift ($\Delta\omega_0$) artifacts from non-uniform B_0 even when the FA of the refocusing pulse was not exactly equal to 180° because of B_1 inhomogeneity.[32,35]

$R_{1\rho}$ dispersion imaging was performed on a 3T Ingenia (Philips Healthcare, Best, The Netherlands) in the sagittal plane, using a 16-channel T/R knee coil that was capable of generating a SL amplitude as high as 1150 Hz, i.e. a maximum B_1~$27\mu T$. Each $R_{1\rho}$-weighted image was acquired using a pair of TSL and ω_1 as listed in Table 1. The key acquisition parameters were as follows: SL 90°/180° RF durations = 0.25/0.5 (ms); FOV = 130*130*96 (mm^3); acquired voxel size = 0.6*0.6*3.0 (mm^3); number of slices = 32;

Compressed SENSE [36] factor = 2.5; fat suppression = "binomial (1-2-1) pulse triplet for α pulse in FLASH readout". The other relevant FLASH parameters were as follows: number of profiles N = 64; TR/TE = 6.8/3.5 (ms); acquisition bandwidth = 573 (Hz/pixel); shot interval = 2 (sec); number of shots (or segments) = 34. An optimal FA of 13° was derived analytically[1,37] given M_{prep}=60%, T_1 =1240 ms[17], TR = 6.8 ms, and N = 64. The phase-encoding order was segmented elliptical centric with outward spiral. One $R_{1\rho}$-weighted 3D image dataset took 1.15 minutes, leading to 9.2 minutes for $R_{1\rho}$ dispersion imaging using a constant M_{prep}.

Three consented volunteers, who were recruited for an IRB-approved clinical study on joint cartilage degeneration, participated in this work. The protocol with M_{prep}=60% was used for the 1st subject with bilateral (asymptomatic) knee scanned, and for the 2nd and the 3rd subjects with unilateral (asymptomatic) knee imaged. To investigate the repeatability of the proposed imaging method, the last two subjects were rescanned after three months.

For comparative purposes, some key acquisition parameters from our previously used standard $R_{1\rho}$ dispersion imaging were provided as follows,[7] i.e. five $\omega_1/2\pi$ settings ranging from 0.125 to 1.0 (kHz); five TSLs from 1 to 40 (ms) per $\omega_1/2\pi$ setting; SL method ="rotary-echo".[29] Compressed SENSE[36] factor = 3.0; TR/TE = 8.5/4.3 (ms); acquisition bandwidth = 382 (Hz/pixel); FA = 10°; acquired voxel size = 0.4*0.4*3.0 (mm^3). Each $R_{1\rho}$ mapping cost 8.75 minutes, and the total scan time for a complete $R_{1\rho}$

dispersion imaging took 43.75 minutes. The success fitting rates (see below) for $R_{1\rho}$ dispersion were respectively 35%, 49%, 36% for the femoral, tibial and patellar cartilage. The fitted model parameters (R_2^i, R_2^a, τ_b and S) can be found in Table 3 from the published paper,[7] which were compared with those derived from the current study using the developed $R_{1\rho}$ dispersion imaging protocol (M_{prep}=60%).

2.3 | Nonlinear least-squares curve fitting

Before quantifying $R_{1\rho}$ dispersion, $R_{1\rho}$-weighted 3D images, including an intra- and an inter-series acquired from each subject's unilateral knee, were co-registered using a free software *elastix*[38] following an established protocol.[23] Then, the femoral, tibial and patellar cartilage were manually outlined using another free software ITK-SNAP,[39] followed by an angular-radial segmentation as previously demonstrated.[23] Note, for the tibial and patellar cartilage, the angular segmentations were evenly partitioned into five ROIs horizontally and vertically. Nonetheless, the radial segmentations were the same for all three knee cartilage compartments. The data analysis was performed on the segmented ROIs in the deep (DZ) and superficial (SZ) zones of cartilage.

Eqs. 1-2 were fitted to average $R_{1\rho}$-weighted voxel values derived from segmented ROIs. The nonlinear least-squares curve fitting was performed using a publicly available IDL script based on the Levenberg-Marquardt algorithm (http://purl.com/net/mpfit).[40] It should be stressed that there were *two independent* variables, i.e. TSL and ω_1, in this unusual data modeling, where four model parameters (i.e. S_0, R_2^i, R_2^a, τ_b) needed to be

optimized. An unweighted fitting was employed in this study, where the uncertainties for each measurable were uniformly set to one. As a result, the output formal 1-sigma fitting errors had to be scaled so that the reduced chi-square χ^2 values were approximately equal to one.[40]

The fitted model parameters were constrained during χ^2 optimizations, i.e. S_0=[100, 1000]; R_2^i =[1, 20] (1/s); R_2^a = [0.5, 100] (1/s) and τ_b= [1, 1000] (μs), with initial values set to 500, 10, 20 and 250, respectively. Given the fitted R_2^a and τ_b, an order parameter S[7] was calculated as $\sqrt{(2R_2^a)/(3d^2\tau_b)}$, with d denoting a constant of 1.028*10^5 (1/s). The uncertainty in S was also derived from the uncertainties of R_2^a and τ_b following the basic error propagation rules.[41] In highly ordered biological tissues, S characterizes an intrinsic property of bound water molecular reorientation anisotropy.[24]

An REF was determined as described before[23] for each of eight $R_{1\rho}$-weighted 3D image datasets, and included in the curve fitting to improve the accuracy of the fits due to an enhanced dynamic range of the measured data. Specifically, these REF signals were considered as those measured using the tailored TSLs (ranging from 13 to 24 ms) and $\omega_1/2\pi$=10 kHz (rather than infinity). As a result, there were 16 measurable data in total for fitting $R_{1\rho}$ dispersion profile of each of the segmented ROIs.

The goodness of fit was loosely defined by R^2, showing how much the observed $R_{1\rho}$ dispersion could be explained by the fitted model.[42] If fitted parameters were within the boundary values and their relative uncertainties did not exceed 100%, the fit was

considered successful otherwise excluded from further analysis. A hit rate (HR%) was defined as the percent of success fits from all the segmented ROIs within each cartilage compartment.

2.4 | Evaluations of $R_{1\rho}$ dispersion quantification

The prepared and the observed M_{prep} were evaluated for potential discrepancies. The proposed imaging protocol was designed with an assumption of R_2^i=R_2^a=20 (1/s), τ_b=300 (μs) for a constant M_{prep}=60%. The average fitted values for each of these model parameters over multiple (n=6) measurements were calculated. Then, the measured M_{prep} dynamic ranges in the DZ and the SZ were determined using eight pairs of TSL and $\omega_1/2\pi$, and compared with the prepared constant M_{prep}.

The duplicated $R_{1\rho}$ dispersion measurements, with a three-month gap on the 2nd and the 3rd subjects, were used to estimate the repeatability of the proposed imaging protocol. This basic statistical assessment, including an intra-subject and an inter-subject repeatability (see below), was performed only in the DZ on the fitted model parameters.

The state-of-the-art $R_{1\rho}$ mapping sequence MAPSS can provide an accurate $R_{1\rho}$ at the cost of doubling scan time.[17] A reference value of $T_{1\rho}$ ($\omega_1/2\pi$=500 Hz) at 3T for each of six standardized segmented compartments in healthy knees (n=7) was documented in Table 2 from the original paper.[43] These $T_{1\rho}$ values were converted into their reciprocals and then an average $R_{1\rho}$ of 24.1±3.8 (1/s) was found for the femoral including trochlea, 27.1±5.1 (1/s) for the tibial and 22.7±1.6 (1/s) for the patellar cartilage.

For comparative purposes, a synthetic $R_{1\rho}$ was calculated using Eq. 2 with $\omega_1/2\pi$=500 Hz and average fitted parameters in Table 2 from the current study. To estimate the precision of the synthetic $R_{1\rho}$, Monte Carlo simulations were performed 1000 runs, each with average fitted parameters (R_2^i, R_2^a and τ_b) contaminated with Gaussian noises.[44] These normally distributed noises were characterized by zero mean and unit variance corresponding to the propagated errors from the DZ and SZ. The means and the standard deviations of 1000 simulated synthetic $R_{1\rho}$ values in different cartilage compartments were compared with the reported references. Following the same procedures, the fitted R_2, i.e. R_2^i+R_2^a, was also compared with those previously reported R_2 at 3T that were measured using the MAPSS sequence in the same publication.[43]

2.5 | Statistical analysis

The coefficient of variation (CV) was used to characterize an intra-subject repeatability of the measureable, calculated for subject *i* (*i=2,3*) as $CV_i = SD_i/M_i$, where the SD_i and M_i denoted the standard deviation and the mean of the measureable from two repeated scans. On the other hand, the root-mean-square of CVs of individual subject, i.e. $CV_{rms} = \sqrt{\sum_{i=1}^{N} CV_i^2/N}$, with N=2, was used to estimate an inter-subject repeatability.[45] Moreover, the stability of the observed M_{prep} was also quantified with CV, and an unpaired t-test was used to assess the differences between two relaxation parameters, with significant difference indicated by $P < .05$. All image and data analysis were performed using

customized software developed in IDL 8.5 (Harris Geospatial Solutions, Inc., Broomfield, CO, USA). All measurements are shown as mean ± standard deviation (SD) unless stated otherwise.

3 | RESULTS

3.1 | An optimized $R_{1\rho}$ dispersion imaging sequence

The proposed $R_{1\rho}$ dispersion imaging sequence is shown schematically in Figure 1, with a fully-refocused SL preparation scheme (a) implemented for a spoiled turbo-FLASH sequence (b). As previously demonstrated, by the numerical simulations and experimental studies at 3T on phantom and the human knee cartilage *in vivo*, the proposed SL scheme was less prone to B_0 and B_1 non-uniform field artifacts particularly at the lower $\omega_1/2\pi$, when compared with the reported SL methods.[35] The prepared constant (red dots) M_{prep} was highlighted in 2D M_{prep} map (c), with respect to the previously used varied (white dots) M_{prep} scheme.

3.2 | Quantitative $R_{1\rho}$ dispersion imaging

The measured (blue filled circles) and modeled (red and green solid lines) representative $R_{1\rho}$ dispersion profiles are demonstrated in Figures 2b-c. The measured data were obtained, as shown in Figure 2a, from a segmented ROI in the tibial deep cartilage (white arrow) and an REF location in the femoral deep cartilage (yellow arrow) of the 1st subject's left knee. The REF data could be easily recognized as the higher signals in Figure 2b and fitted by a straight (green) line because there was hardly any $R_{1\rho}$ dispersion around the magic angle

locations. These REF data were absent in Figure 2c because they ($\omega_1/2\pi$=10 kHz) were out of the display range.

The success fitting or hit rates (HR%) using the constant M_{prep} (60%) were much higher than those with the varied M_{prep};[7] specifically, they were respectively 72% vs. 35% (femoral), 87% vs. 49% (tibial), and 59% vs. 36% (patellar). Figure 3 presents an example of $R_{1\rho}$ dispersion quantification from the 3rd subject's knee. An anatomical T1ρW sagittal image slice is shown (Fig. 3a) superimposed with segmented ROIs. The ROI-based parametric color maps, i.e. R_2^i (Fig. 3b), R_2^a (Fig. 3c), τ_b (Fig. 3d), S (Fig. 3e) and R^2 (Fig. 3f), were overlaid on the T1ρW image.

Around the trochlear cartilage as indicated by a white arrow in Fig. 3f, the decreased R^2 values revealed less reliable $R_{1\rho}$ dispersion quantification, probably resulting from a vanishing residual dipolar interaction near the magic angle orientation. It was challenging to manually segment the DZ precisely near the calcified cartilage;[46] hence, it was no surprising to observe some abrupt R_2^a changes as shown in the deep femoral cartilage as shown in Fig. 3c. However, an unusual high R_2^a in the deep tibial cartilage, as indicated by yellow arrows in Figs. 3a and 3c, might not be well accounted for by an inaccurate segmentation. Both T2W (not shown) and T1ρW images showed relatively low signals on that particular tibial cartilage location, suggesting that the corresponding R_2^a relaxation was enhanced as the R_2^i relaxation (Fig. 3b) was relatively uniform across the tibial cartilage.

3.3 | Developed and previous $R_{1\rho}$ dispersion imaging

Figure 4 compares the average fitted R_2^i (Fig. 4a), R_2^a (Fig. 4b), τ_b (Fig. 4c) and S (Fig. 4d) over six measurements in the DZ (red) and the SZ (green) using the developed $R_{1\rho}$ dispersion imaging protocol on three subjects, with those from the previously reported in the DZ* (blue) using the standard method on one subject,[7] in the femoral, tibial and patellar cartilage compartments.

The fitted values with the proposed protocol are also tabulated in Table 2, showing that the fits in the DZ were comparable with (i.e. R_2^i), smaller than (i.e. τ_b) and larger (i.e. R_2^a and S) than those in the SZ. When compared with the fits (red) from this work, the previously reported (blue) R_2^a (1/s) was significantly reduced in the femoral (11.3±4.9 vs. 22.0±3.1, P=.01) and tibial (8.7±4.1 vs. 39.1±8.9, P<.01) cartilage while the R_2^i (1/s) was not significantly (P>.33) different across all three cartilage compartments. On average, the previously reported τ_b and S values were respectively about twice and half of those from the current study.

3.4 | Measured dynamic range of M_{prep}

Given the fitted R_2^i, R_2^a and τ_b in Table 2, the measured M_{prep} was calculated using eight combinations of TSL and $\omega_1/2\pi$ for M_{prep}=60% (Table 1), and plotted for the SZ (Figure 5a) and the DZ (Figure 5b) in the femoral (red), tibial (green) and patellar (blue) cartilage. Although some observed M_{prep} profiles considerably deviated from an initially designed M_{prep} (dashed lines), the variations of these measured M_{prep} were rather relatively small,

e.g. with a CV of 8.3% in the deep tibial cartilage and of 1.3% in the superficial patellar cartilage.

3.5 | Precision and accuracy assessments

The values of CV and CV_{rms} for the fitted parameters (R_2^i, R_2^a, τ_b, S) were calculated. For Subject 2, the proposed $R_{1\rho}$ dispersion imaging protocol had provided a relatively precise measurement as indicated by an average intra-subject repeatability of CV_2=4.2±2.1% for all fitted parameters over the whole cartilage. This observation was generally in line with an average inter-subject repeatability of CV_{rms}=4.6±2.5% as shown in Figure 5c, when excluding those τ_b and S values in the patellar cartilage. It was unclear why CV_3 (from Subject 3) of the fitted parameters for the repeated scans were markedly diversified only in the patellar cartilage.

Nonetheless, the differences between the synthetic $R_{1\rho}$ (1/s) (gold) and the references[43] from MAPSS (blue), as revealed in Figure 6a, were not statistically significant in the femoral (23.0±5.3 vs. 24.1±3.8, *P*=.67) and tibial (29.1±8.8 vs. 27.1±5.1, *P*=.62) cartilage, but that was not the case in the patellar (16.5±4.9 vs. 22.7±1.6, *P*=.01) cartilage. Meanwhile, the synthetic $R_{1\rho}$ appeared less precise (i.e. with larger SDs) with respect to the reported. The same trend, as shown in Figure 6b, was also observed when comparing the fitted R_2 (1/s) (gold) with the references[43] (blue), in the femoral (29.7±5.1 vs. 32.4±4.9, *P*=.34, tibial (38.7±10.1 vs. 36.4±7.4, *P*=.66) and patellar (23.5±6.3 vs. 32.5±2.2, *P*<.01) cartilage.

4 | DISCUSSION

4.1 | General comments

An efficient acquisition method for $R_{1\rho}$ dispersion imaging of the human knee cartilage at 3T has been developed in this work. The basic idea is to prepare the constant $R_{1\rho}$-weighting by simultaneously tailoring TSL and ω_1 in a spoiled turbo-FLASH sequence. This unique method not only markedly reduces the total acquisition time but also alleviates the potential T_1 relaxation artifacts during FLASH imaging readout in the standard $R_{1\rho}$ mapping. The measurement results from repeated scans and from comparisons with the literature suggest that the proposed imaging method is a promising tool to further explore $R_{1\rho}$ dispersion in the human knee cartilage in clinical settings.

4.2 | Improved acquisition efficiency on $R_{1\rho}$ dispersion imaging

The primary advantage of the proposed method relies on its acquisition efficiency, making it feasible to be employed in clinical studies. Traditionally, it took an unrealistically long scan time to collect multiple series of $R_{1\rho}$-weighted images with different ω_1. For instance, the first such study of *in vivo* human knee cartilage utilized 12 different ω_1, with each ω_1 setting for $R_{1\rho}$ mapping lasting more than 5 minutes using 5 different TSLs, resulting in the total scan time of more than 1 hour.[25] Similarly, our previous standard $R_{1\rho}$ dispersion imaging protocol cost about 45 minutes using 5 ω_1, with each ω_1 for 5 TSL settings.[7]

By contrast, the proposed $R_{1\rho}$ dispersion imaging protocol took only 9.2 minutes for eight constant $R_{1\rho}$-weighted images, and this practical acquisition time could be even

shortened further by reducing the number of the acquired $R_{1\rho}$ weightings. There are only 4 model parameters (i.e. S_0, R_2^i, R_2^a and τ_b, with R_2^{ex}=0) as shown in Eqs. 1-2, and thus two acquisitions would suffice to determine these parameters given two extra REFs. In fact, this concept has been exploited in our previous work to derive an anisotropic R_2^a from a single T_2-weighed image.[23] Nonetheless, it would be unwise to characterize $R_{1\rho}$ dispersion using only two acquisitions just as to quantify $R_{1\rho}$ itself using two time points. This becomes a question of the trade-off between accuracy and efficiency – a topic beyond the scope of this study.

In principle, the prepared SL magnetization could be readout using any fast imaging sequence, for instance, turbo spin echo sequence (TSE). One possible reason for an argument to favor TSE, rather than FLASH, would be its immunity to the potential B_0 field inhomogeneity. However, the potential SAR constraints at 3T with TSE most likely would slow down its intrinsic speed in clinical applications. Without any concerns of the SAR issues, the employed turbo FLASH sequence in the proposed $R_{1\rho}$ dispersion acquisition had been demonstrated nearly as efficient as EPI.[37]

While the implemented spin-lock scheme has been demonstrated to be less prone to the image artefacts associated with non-uniform B_0 and B_1 fields,[32,35] the deviations of actual B_1 fields from the prescribed ones might have an adverse effect on the accuracy of $R_{1\rho}$ dispersion quantification particularly on the edged imaging slices in the human knee where the B_1 inhomogeneity (i.e. ΔB_1) usually becomes deteriorated. In the literature,[47]

ΔB_1 has been demonstrated to be relatively small (~5%) in the human knee cartilage and our previous B_1 mapping (data not shown) was largely consistent with the literature. Nonetheless, it would be of great interest to further investigate to what extent the B_1 mapping could increase the accuracy of $R_{1\rho}$ dispersion quantification in clinical studies.

4.3 | Spin-lock prepared constant M_{prep}

The constant M_{prep} was calculated with the assumed values of R_2^i, R_2^a and τ_b, inferred from the literature.[25] It was impossible for the whole cartilage to have a constant M_{prep} across various locations because of an orientation-dependent R_2^a. Nonetheless, if the prepared M_{prep} had been clustered in a narrow range, the expected k-space filtering effect would have been comparable for each segmented acquisition in phase-encoding directions, thus diminishing an adverse T_1 relaxation effect during FLASH imaging readout.[27]

As shown in Figs. 5a-b, some observed M_{prep} values for different cartilage locations significantly deviated from the designed 60%; however, they were all maintained within a limited dynamic range. It was the variation rather than the absolute value of M_{prep} that had played a key role in imparting the k-space filtering effect on quantifying $R_{1\rho}$. This observation suggests that the precise values of R_2^i, R_2^a and τ_b might not be as essential as initially thought for tailoring a constant M_{prep} in $R_{1\rho}$ dispersion imaging.

As a reference, the prepared M_{prep} using the standard $R_{1\rho}$ dispersion imaging protocol was provided herein, with a range from 98% ($\omega_1/2\pi$=1 kHz and TSL=1 ms) to 23% ($\omega_1/2\pi$=125 Hz and TSL= 40 ms) given that R_2^i=R_2^a=20 (1/s), τ_b=300 (μs). It was

no surprising then that quantification of $R_{1\rho}$ dispersion became unreliable even without considering the robustness of spin-lock[7,35] or the possibility of involuntary knee movements when using this lengthy imaging protocol.

4.4 | Quantifying $R_{1\rho}$ dispersion with an REF

The key to the success of $R_{1\rho}$ dispersion quantification depends on integrating an additional information derived from the MA location in the deep femoral cartilage. This is because the prepared M_{prep} was intended to be constant; in other words, the dynamic range in M_{prep} was limited thus leading to unreliable data fitting. Our previous study has documented on how to accurately extract an REF in the deep femoral cartilage,[23] and the defined REF was also applied to the tibial and patellar cartilage in this work, with an assumption of the comparable S_0 and R_2^i values across the whole knee cartilage.

Based on the comparison results with the gold standards in Figure 6, it was challenging to positively corroborate this assumption in the current work because of inconsistent results observed in the tibial and patellar cartilage. However, the measured $R_{1\rho}$ and R_2 in the tibial from both methods were constantly higher than those in the femoral and patellar cartilage, reflective of the fact in that the majority of collagen fibers in the tibial cartilage are along with B_0. This interesting finding is in accordance with the literature albeit unspecified.[48]

4.5 | Precision and accuracy of $R_{1\rho}$ dispersion quantification

When excluding some CV_3 for the fitted values (R_2^a, τ_b and S) in the patellar cartilage of the 3rd subject, the precision of $R_{1\rho}$ dispersion measurements seems reasonably good. However, it was still unclear why the repeated scans on the 3rd subject's knee did not produce the comparable results only in the patellar cartilage. This observation could not be fully accounted for by an imperfect acquisition protocol. Nonetheless, an informative test of the proposed $R_{1\rho}$ dispersion imaging method was to compare its results with those measured using the state-of-the-art $R_{1\rho}$ mapping sequence (MAPSS).[17]

The observed comparable average $R_{1\rho}$ in the femoral and tibial cartilage (Fig. 6a) lend strong support to that not only was the proposed method efficient but it was also robust in quantifying $R_{1\rho}$ dispersion. It is worth emphasizing that the acquisitions and analyses methods used in the two measurements were fundamentally different, yet the comparable $R_{1\rho}$ values were still attained. The 3rd subject had inconsistent measurement results between two repeated scans in the patellar cartilage, which could be partially responsible for the observed $R_{1\rho}$ deviation from the reference.

Another interesting observation was that the synthetic $R_{1\rho}$ had a relatively larger variation than those based on the MAPSS sequence. It could be the case that the uncertainty of the synthetic $R_{1\rho}$ had been overestimated through multiple-step error propagations. At least one parameter (i.e. R_2^a) had its variation not completely accounted for with the random Gaussian noises because it was orientation dependent. Further investigations are needed to better understand the observed $R_{1\rho}$ discrepancies with respect to the reported references.

Although comparable values (Fig. 6b) were also attained between our fitted R_2 and the references, caution should be exercised when interpreting the comparative results. The R_2 references were actually acquired using a combination of CPMG preparation and MAPSS readout.[49] The reported R_2 from healthy control (n=7) knee cartilage at 3T and 7T were comparable[43] indicative of hardly any chemical exchange effect contribution to R_2 at 7T, which is apparently inconsistent with the literature.[50,51] It remains unclear to what extent the previously reported R_2 at 3T had been compromised by the CPMG-based magnetization preparation possibly due to a nontrivial spin-locking effect.[52]

4.6 | Limitations

The current work has some limitations. First, no effort had been devoted to separating the factors contributing to the improved success fitting rates for the measured $R_{1\rho}$ dispersion profiles. These factors might comprise a fully-refocused SL preparation and a limited dynamic range in the spin-lock prepared magnetizations for turbo-FLASH imaging readout. Second, there was no gold standard for an internal reference used in this study, and thus it became unclear to what extent the reported $R_{1\rho}$ dispersion parameters could have been compromised. Third, the longitudinal magnetization at the end of FLASH readout was not spoiled, potentially leading to signal inconsistencies among initial spin-lock magnetization preparations. The magnetization reset pulses as employed in MAPSS[17] could be implemented for the developed $R_{1\rho}$ dispersion pulse sequence. Fourth, only a small number of subjects were involved in this study, and data from additional subjects would

provide an increased statistical power to support the conclusions. Fifth, the analysis of $R_{1\rho}$ dispersion may be unreliable for some locations in the femoral and patellar cartilage in which the residual dipolar coupling approached zero near the MA orientation. Last, it has been revealed that the contralateral healthy knee may also exhibit molecular changes after ipsilateral knee injury;[53] hence, some changes observed between the repeated scans might be "real" and not attributable to the imaging protocol.

5 | CONCLUSIONS

We have developed a practical $R_{1\rho}$ dispersion imaging protocol for clinical studies of *in vivo* human knee cartilage at 3T, which has been demonstrated not only efficient but also robust. Although this proposed method was developed for joint cartilage, its underlying principle could be applied to other biological tissues with $R_{1\rho}$ dispersion properties regardless of relaxation mechanisms.

ACKNOWLEDGEMENTS

We would like to thank Prof. Thomas Chenevert for support and encouragement, and Suzan Lowe and James O'Connor for help in collecting human knee images. This work was in part supported by the Eunice Kennedy Shriver National Institute of Child Health & Human Development of the National Institutes of Health (NIH) under Award Number R01HD093626 (to Prof. Riann Palmieri-Smith) and a Discovery Grant by the University of Michigan – Peking University Health Science Center (UM-PUHSC) Joint Institute (to

Prof. Tristan Maerz). The content is solely the responsibility of the authors and does not necessarily represent the official views of the NIH.

DATA AVAILABILITY STATEMENT

Data available on request from the authors.

REFERENCES

1. Vlaardingerbroek MT, Boer JA. *Magnetic resonance imaging: theory and practice.* Springer Science & Business Media; 2013.
2. Mathur-De Vre R. The NMR studies of water in biological systems. *Progress in Biophysics and Molecular Biology.* 1980;35:103-134.
3. Woessner DE. Nuclear magnetic-relaxation and structure in aqueous heterogenous systems. *Mol Phys.* 1977;34(4):899-920.
4. Peto S, Gillis P, Henri VP. Structure and dynamics of water in tendon from NMR relaxation measurements. *Biophysical journal.* 1990;57(1):71-84.
5. Knispel RR, Thompson RT, Pintar MM. Dispersion of proton spin-lattice relaxation in tissues. *J Magn Reson.* 1974;14(1):44-51.
6. Duvvuri U, Goldberg AD, Kranz JK, et al. Water magnetic relaxation dispersion in biological systems: The contribution of proton exchange and implications for the noninvasive detection of cartilage degradation. *P Natl Acad Sci USA.* 2001;98(22):12479-12484.
7. Pang Y. An order parameter without magic angle effect (OPTIMA) derived from R1ρ dispersion in ordered tissue. *Magn Reson Med.* 2020;83(5):1783-1795.
8. Borthakur A, Mellon E, Niyogi S, Witschey W, Kneeland JB, Reddy R. Sodium and T1ρ MRI for molecular and diagnostic imaging of articular cartilage. *NMR Biomed.* 2006;19(7):781-821.
9. Reddy R, Insko EK, Kaufman JH, Bolinger L, Kneeland JB, Leigh JS. MR imaging of cartilage under spin-locking. In: Proceedings of the 3rd Annual Meeting of ISMRM, Nice, France, 1995. (abstract: 1535).
10. Wang L, Regatte RR. T(1)rho MRI of human musculoskeletal system. *J Magn Reson Imaging.* 2015;41(3):586-600.
11. Link TM, Neumann J, Li X. Prestructural Cartilage Assessment Using MRI. *J Magn Reson Imaging.* 2017;45(4):949-965.
12. Link TM, Li X. Establishing compositional MRI of cartilage as a biomarker for clinical practice. *Osteoarthritis and Cartilage.* 2018;26(9):1137-1139.

13. Kim J, Mamoto K, Lartey R, et al. Multi-vendor multi-site T1ρ and T2 quantification of knee cartilage. *Osteoarthritis and Cartilage.* 2020;28(12):1539-1550.
14. Jones GP. Spin-lattice relaxation in the rotating frame: weak-collision case. *Physical Review.* 1966;148(1):332-335.
15. Akella SVS, Regatte RR, Gougoutas AJ, et al. Proteoglycan-induced changes in T-1 rho-relaxation of articular cartilage at 4T. *Magnet Reson Med.* 2001;46(3):419-423.
16. Regatte RR, Akella SVS, Lonner JH, Kneeland JB, Reddy R. T-1p relaxation mapping in human osteoarthritis (OA) cartilage: Comparison of T-1p with T-2. *Journal of Magnetic Resonance Imaging.* 2006;23(4):547-553.
17. Li X, Han ET, Busse RF, Majumdar S. In vivo T(1rho) mapping in cartilage using 3D magnetization-prepared angle-modulated partitioned k-space spoiled gradient echo snapshots (3D MAPSS). *Magn Reson Med.* 2008;59(2):298-307.
18. Regatte RR, Akella SV, Borthakur A, Kneeland JB, Reddy R. Proteoglycan depletion–induced changes in transverse relaxation maps of cartilage: comparison of T2 and T1ρ. *Academic radiology.* 2002;9(12):1388-1394.
19. van Tiel J, Kotek G, Reijman M, et al. Is T1rho Mapping an Alternative to Delayed Gadolinium-enhanced MR Imaging of Cartilage in the Assessment of Sulphated Glycosaminoglycan Content in Human Osteoarthritic Knees? An in Vivo Validation Study. *Radiology.* 2016;279(2):523-531.
20. Shao H, Pauli C, Li S, et al. Magic angle effect plays a major role in both T1rho and T2 relaxation in articular cartilage. *Osteoarthritis Cartilage.* 2017;25(12):2022-2030.
21. Menezes NM, Gray ML, Hartke JR, Burstein D. T2 and T1rho MRI in articular cartilage systems. *Magn Reson Med.* 2004;51(3):503-509.
22. Mlynarik V, Szomolanyi P, Toffanin R, Vittur F, Trattnig S. Transverse relaxation mechanisms in articular cartilage. *J Magn Reson.* 2004;169(2):300-307.
23. Pang Y, Palmieri-Smith RM, Malyarenko DI, Swanson SD, Chenevert TL. A unique anisotropic R2 of collagen degeneration (ARCADE) mapping as an efficient alternative to composite relaxation metric (R2 -R1 rho) in human knee cartilage study. *Magn Reson Med.* 2019;81(6):3763-3774.
24. Lenk R, Bonzon M, Greppin H. Dynamically oriented biological water as studied by NMR. *Chemical Physics Letters.* 1980;76(1):175-177.
25. Wang P, Block J, Gore JC. Chemical exchange in knee cartilage assessed by R1rho (1/T1rho) dispersion at 3T. *Magn Reson Imaging.* 2015;33(1):38-42.
26. Coremans J, Spanoghe M, Budinsky L, et al. A comparison between different imaging strategies for diffusion measurements with the centric phase-encoded turboFLASH sequence. *J Magn Reson.* 1997;124(2):323-342.

27. Williams CF, Redpath TW. Sources of artifact and systematic error in quantitative snapshot FLASH imaging and methods for their elimination. *Magnetic Resonance in Medicine: An Official Journal of the International Society for Magnetic Resonance in Medicine.* 1999;41(1):63-71.
28. Chen W. Errors in quantitative T1rho imaging and the correction methods. *Quant Imag Med Surg.* 2015;5(4):583-591.
29. Charagundla SR, Borthakur A, Leigh JS, Reddy R. Artifacts in T-1 rho-weighted imaging: correction with a self-compensating spin-locking pulse. *J Magn Reson.* 2003;162(1):113-121.
30. Mitrea BG, Krafft AJ, Song RT, Loeffler RB, Hillenbrand CM. Paired self-compensated spin-lock preparation for improved T-1 rho quantification. *J Magn Reson.* 2016;268:49-57.
31. Zeng H, Danie lG, Gochberg C, Zhao Y, Avison M, Gore JC. A composite spin-lock pulse for ΔB0 + B1 insensitive T1rho measurement. In: Proceedings of the 14th Annual Meeting of ISMRM, Seattle, Washington, USA, 2006. (abstract: 2356).
32. Gram M, Seethaler M, Gensler D, Oberberger J, Jakob PM, Nordbeck P. Balanced spin‐lock preparation for B1‐insensitive and B0‐insensitive quantification of the rotating frame relaxation time T1ρ. *Magnet Reson Med.* 2020.
33. Johnson CP, Thedens DR, Kruger SJ, Magnotta VA. Three‐Dimensional GRE T1ρ mapping of the brain using tailored variable flip‐angle scheduling. *Magnet Reson Med.* 2020.
34. Momot KI, Pope JM, Wellard RM. Anisotropy of spin relaxation of water protons in cartilage and tendon. *NMR Biomed.* 2010;23(3):313-324.
35. Pang Y. A self-compensated spin-locking scheme for quantitative R1ρ dispersion in articular cartilage. In: Proceedings of the 28th Annual Meeting of ISMRM, Paris, France, 2020. (abstract: 2743).
36. Geerts-Ossevoort; L, Weerdt; Ed, Duijndam; A, et al. Compressed SENSE. Speed done right. Every time. https://philipsproductcontent.blob.core.windows.net/assets/20180109/619119731f2a42c4acd4a863008a46c7.pdf. 2018; https://philipsproductcontent.blob.core.windows.net/assets/20180109/619119731f2a42c4acd4a863008a46c7.pdf. Accessed 09/20, 2019.
37. Norris DG. Excitation angle optimization for snapshot FLASH and a signal comparison with EPI. *Journal of Magnetic Resonance (1969).* 1991;91(1):190-193.
38. Klein S, Staring M, Murphy K, Viergever MA, Pluim JPW. elastix: A Toolbox for Intensity-Based Medical Image Registration. *Ieee T Med Imaging.* 2010;29(1):196-205.

39. Yushkevich PA, Piven J, Hazlett HC, et al. User-guided 3D active contour segmentation of anatomical structures: significantly improved efficiency and reliability. *Neuroimage.* 2006;31(3):1116-1128.
40. Markwardt CB. "Non-linear least-squares fitting in IDL with MPFIT", in proc. Astronomical Data Analysis Software and Systems XVIII, Quebec, Canada, ASP Conference Series, Vol. 411, eds. D. Bohlender, P. Dowler & D. Durand (Astronomical Society of the Pacific: San Francisco), p. 251-254. 2009.
41. Bevington PR, Robinson DK. *Data reduction and error analysis for the physical sciences.* 3rd ed. Boston: McGraw-Hill; 2003.
42. Motulsky HJ, Ransnas LA. Fitting curves to data using nonlinear regression: a practical and nonmathematical review. *The FASEB journal.* 1987;1(5):365-374.
43. Wyatt C, Guha A, Venkatachari A, et al. Improved differentiation between knees with cartilage lesions and controls using 7T relaxation time mapping. *J Orthop Transl.* 2015;3(4):197-204.
44. Press WH, Teukolsky SA, Vetterling WT, Flannery BP. Numerical recipes in C. Cambridge university press Cambridge; 1988.
45. Sharafi A, Chang G, Regatte RR. Biexponential T2 relaxation estimation of human knee cartilage in vivo at 3T. *Journal of Magnetic Resonance Imaging.* 2018;47(3):809-819.
46. Mahar R, Batool S, Badar F, Xia Y. Quantitative measurement of T2, T1ρ and T1 relaxation times in articular cartilage and cartilage-bone interface by SE and UTE imaging at microscopic resolution. *J Magn Reson.* 2018;297:76-85.
47. Wang L, Schweitzer ME, Padua A, Regatte RR. Rapid 3D-T(1) mapping of cartilage with variable flip angle and parallel imaging at 3.0T. *J Magn Reson Imaging.* 2008;27(1):154-161.
48. Razmjoo A, Caliva F, Lee J, et al. T2 analysis of the entire osteoarthritis initiative dataset. *Journal of Orthopaedic Research®.* 2020.
49. Li X, Wyatt C, Rivoire J, et al. Simultaneous acquisition of T1rho and T2 quantification in knee cartilage: repeatability and diurnal variation. *J Magn Reson Imaging.* 2014;39(5):1287-1293.
50. Welsch GH, Apprich S, Zbyn S, et al. Biochemical (T2, T2* and magnetisation transfer ratio) MRI of knee cartilage: feasibility at ultra-high field (7T) compared with high field (3T) strength. *European radiology.* 2011;21(6):1136-1143.
51. Jordan CD, Saranathan M, Bangerter NK, Hargreaves BA, Gold GE. Musculoskeletal MRI at 3.0 T and 7.0 T: a comparison of relaxation times and image contrast. *European journal of radiology.* 2013;82(5):734-739.
52. Santyr GE, Henkelman RM, Bronskill MJ. Variation in measured transverse relaxation in tissue resulting from spin locking with the CPMG sequence. *Journal of Magnetic Resonance (1969).* 1988;79(1):28-44.

53. Ochoa J, Amano K, Tanaka M, et al. Altered biomechanics and cartilage health changes in bilateral knees following unilateral ACL reconstruction: a 2-year follow-up. *Osteoarthritis and Cartilage*. 2016;24:S406-S407.

SIX FIGURES

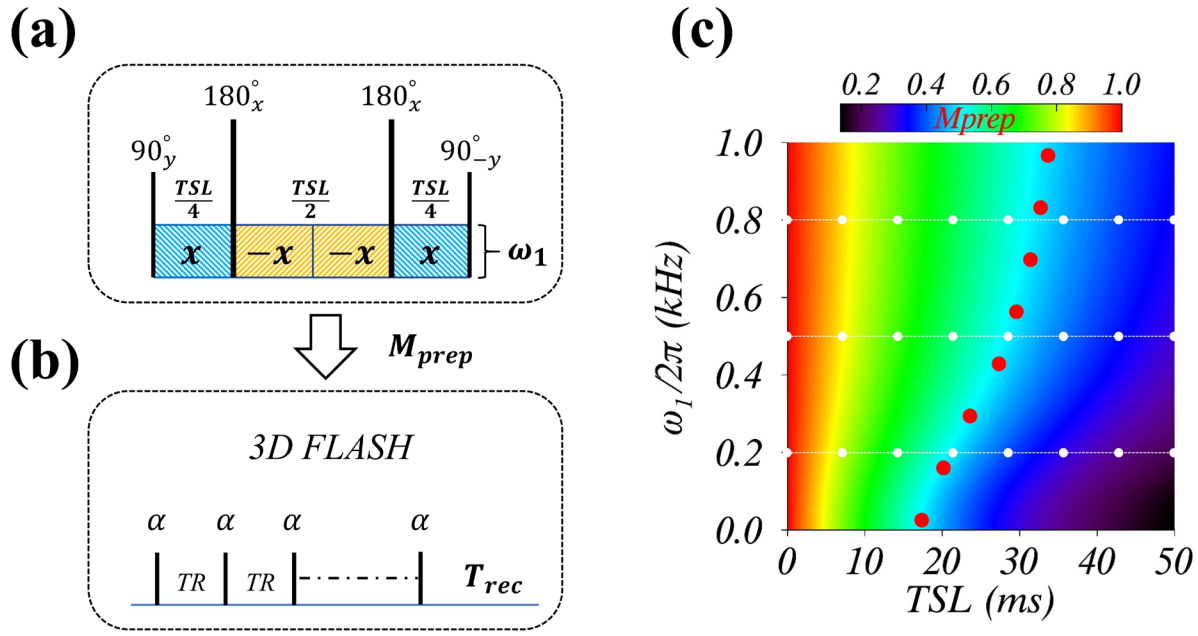

FIGURE 1. Schematic of the proposed $R_{1\rho}$ dispersion imaging sequence including a fully-refocused SL preparation (a) for a spoiled turbo-FLASH readout (b), and a prepared constant (red

dots) SL magnetizations M_{prep} (c). FLASH, fast low angle shot; SL, spin-lock; TSL, spin-lock time; ω_1, spin-lock RF amplitude.

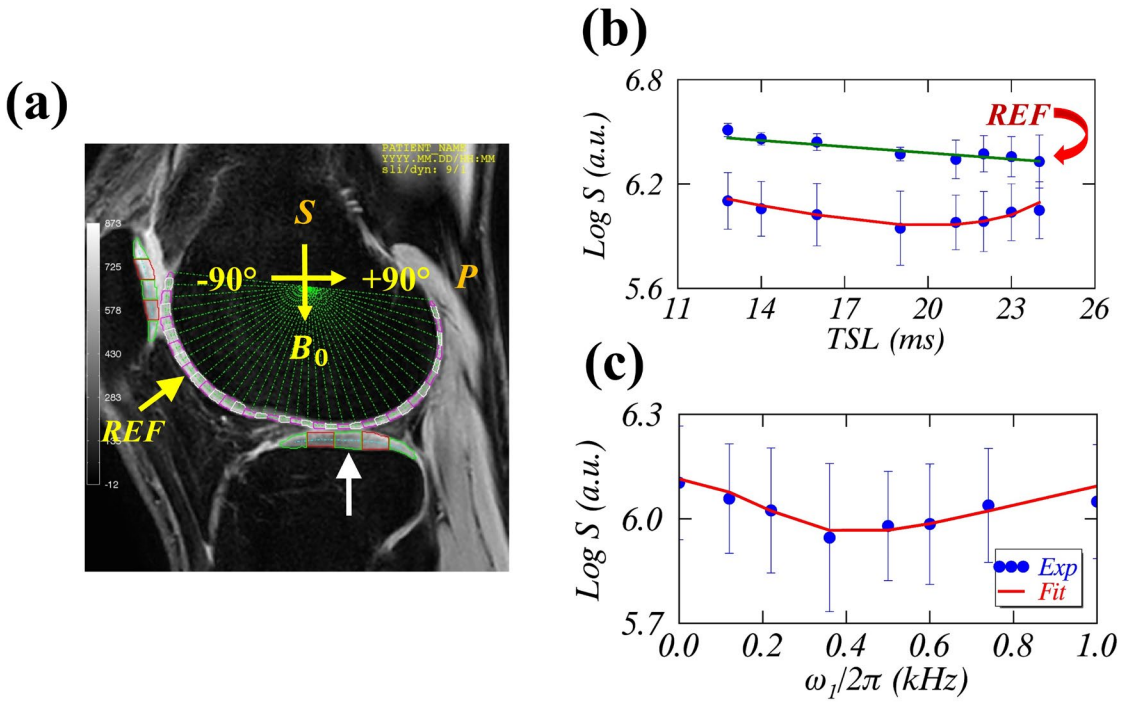

FIGURE 2. Measured (blue filled circles) and fitted (red and green solid lines) exemplary $R_{1\rho}$ dispersion profile vs. TSL (b) and $\omega_1/2\pi$ (c). The presented $R_{1\rho}$-weighted signals were measured from one segmented ROI in the deep tibial cartilage (white arrow), and the REF data were taken from the deep femoral cartilage (yellow arrow) as shown (a). DZ, deep zone; P, posterior; REF, internal reference; ROI, region of interest; S, superior; TSL, spin-lock time; ω_1, spin-lock amplitude.

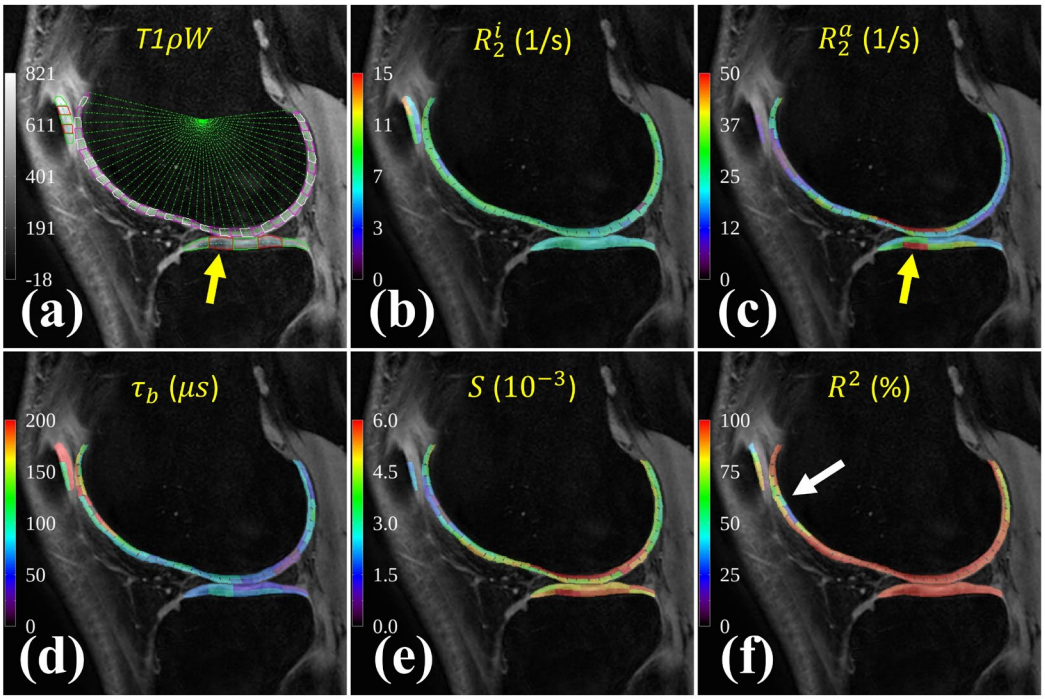

FIGURE 3. Representative ROI-based parametric color maps of R_2^i (b), R_2^a (c), τ_b (d), S (e) and R^2 (f) derived from $R_{1\rho}$ dispersion imaging of the 3rd subject's knee, each superimposed on one T1ρW sagittal image (a). ROI, region of interest; μs, microsecond.

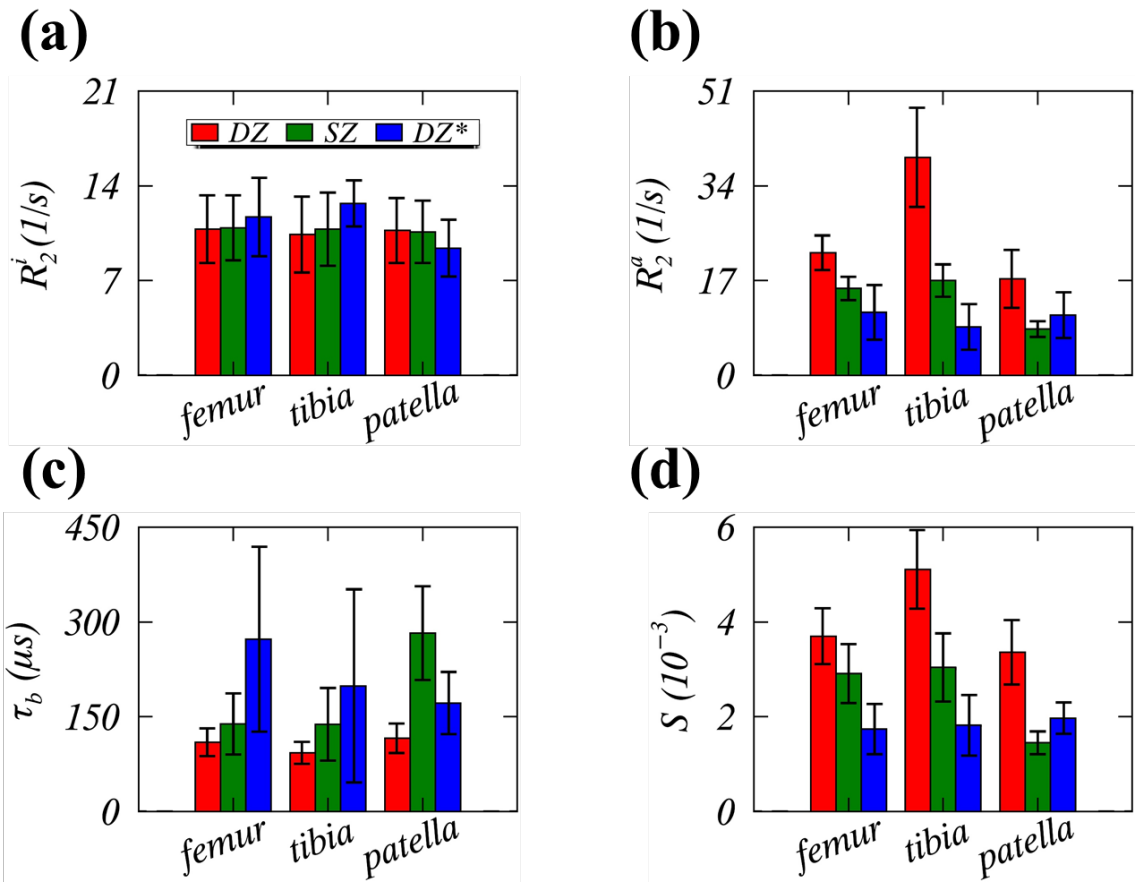

FIGURE 4. Averaged over six measurements from three subjects, the fitted parameters of R_2^i (a), R_2^a (b), τ_b (c), S (d) were compared in the DZ (red) and the SZ (green) of all three cartilage compartments. Also included were the related values (blue) in the deep zone (DZ*) derived from the previous standard $R_{1\rho}$ dispersion imaging. DZ, deep zone; SZ, superficial zone.

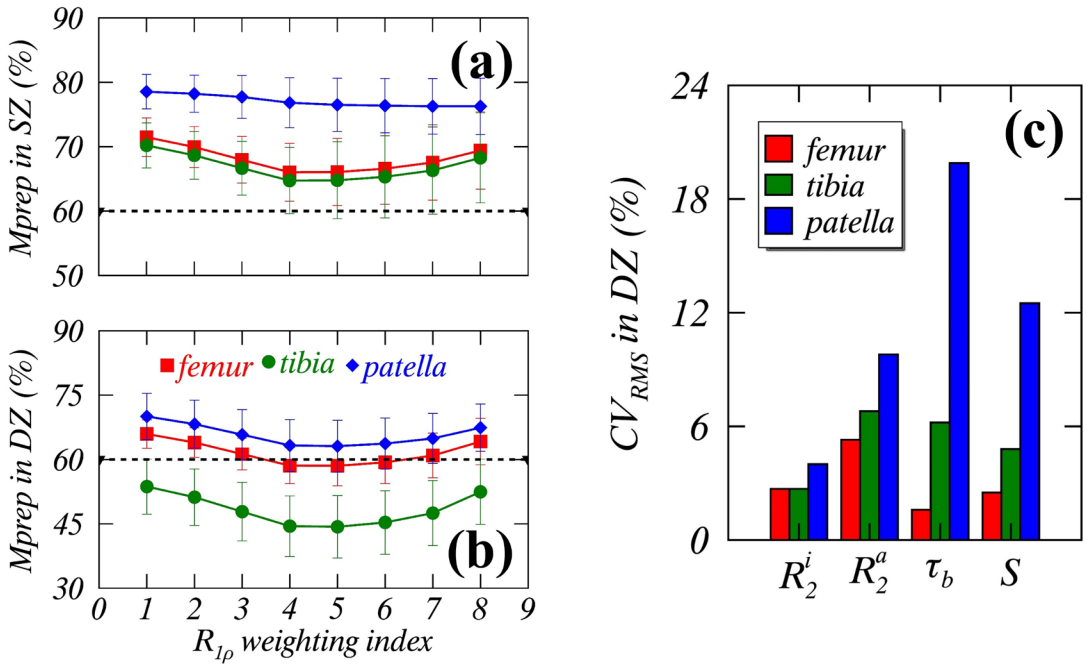

FIGURE 5. Measured average M_{prep} in the SZ (a) and the DZ (b) of the femoral (red), tibial (green) and patellar (blue) cartilage compartments. The tailored M_{prep} was indicated by a horizontal dashed line. Inter-subject repeatability measures were compared (c) for the fitted parameters $(R_2^i, R_2^a, \tau_b, S)$ in the deep femoral (red), tibial (green) and patellar (blue) cartilage compartments. DZ, deep zone; M_{prep}, spin-lock prepared magnetization; SZ, superficial zone.

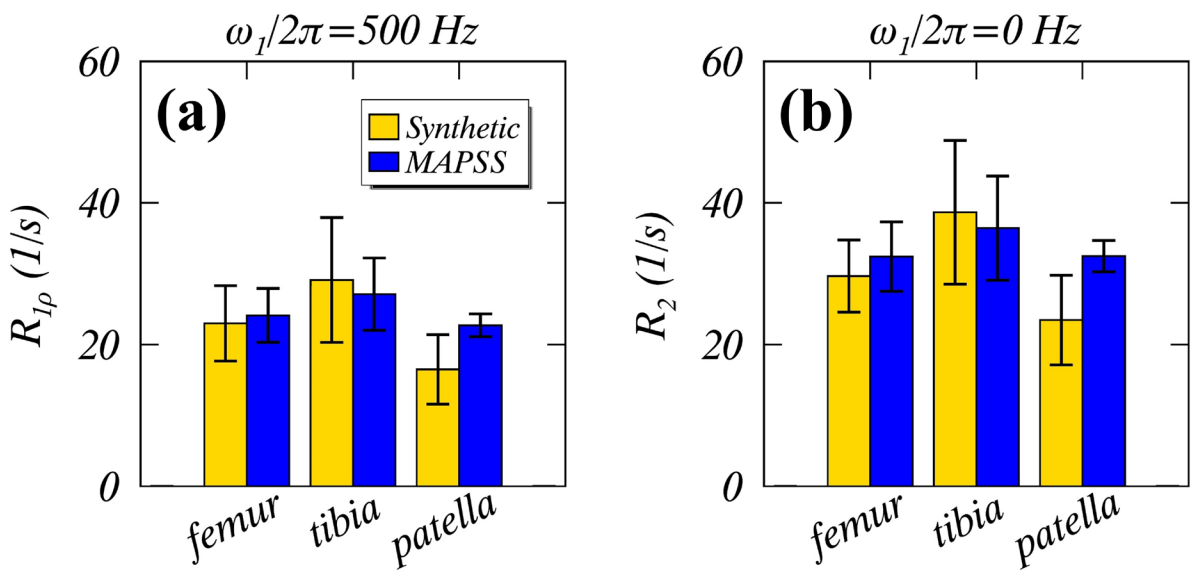

FIGURE 6. Average synthetic (gold) $R_{1\rho}$ (a) and R_2 (b), compared with the references (blue) measured using MAPSS sequences in all three cartilage compartments. MAPSS, magnetization-prepared angle-modulated partitioned k-space spoiled gradient echo snapshots; ω_1, spin-lock RF amplitude. The presented $R_{1\rho}$ and R_2 data with MAPSS were extracted from Reference (43)

TWO TABLES

TABLE 1. A constant prepared spin-lock magnetization (M_{prep}=60%) with eight pairs of spin-lock RF durations (TSL) and amplitudes ($\omega_1/2\pi$). These tailored settings were based on $R_2^i = R_2^a = 20$ (1/s), τ_b=300 (μs) and R_2^{ex}=0.

Scan index	1	2	3	4	5	6	7	8

TSL (ms)	13	14	16	19	21	22	23	24
$\omega_1/2\pi$ (Hz)	0	120	220	360	500	600	740	1000

TABLE 2. Average success fitting rates (HR%) and average fitted model parameters over six $R_{1\rho}$ dispersion measurements (M_{prep}=60%) on three subjects in the DZ and the SZ within the femoral, tibial and patellar cartilage compartments. DZ, deep zone; M_{prep}, spin-lock prepared magnetization; SZ, superficial zone.

Fits	DZ			SZ		
	femoral	*tibial*	*patellar*	*femoral*	*tibial*	*patellar*
HR (%)	71.7±12.3	87.2±8.9	58.6±13.5	66.2±10.4	90.1±9.4	21.1±13.6
R_2^i *(1/s)*	10.8±2.5	10.4±2.8	10.7±2.4	10.9±2.4	10.8±2.7	10.6±2.3
R_2^a *(1/s)*	22.0±3.1	39.1±8.9	17.3±5.2	15.6±2.1	17.0±2.9	8.3±1.4
τ_b *(μs)*	109.7±22.0	92.8±17.3	115.8±23.3	138.7±48.3	138.1±57.4	282.2±74.2
S (10^{-3})	3.70±0.59	5.11±0.83	3.36±0.68	2.91±0.62	3.04±0.72	1.45±0.24